PAPER

Tailoring the antibacterial and antioxidant activities of iron nanoparticles with amino benzoic acid

Shah Faisal,[a] Saima Sadiq,[d] Muhammad Mustafa,[a] Muhammad Hayat Khan,[a] Muhammad Sadiq, [iD] *[a] Zaffar Iqbal[b] and Maham Khan[c]

Antibacterial resistance is a massive universal health crisis and one of the most significant threats to human life. Many bacterial species have evolved and obtained resistance against multiple drugs. As a result, alternative antibacterial agents are essentially required to fight infections caused by resistant pathogenic bacteria. To study the antibacterial activity of iron nanoparticles against methicillin-resistant *Staphylococcus aureus*, the nanoparticles were synthesized *via* the microwave induced precipitation method using an aqueous solution of ferric and ferrous ions (1 : 1.5) M with sodium hydroxide (3 M). The antibacterial activity of iron nanoparticles was compared with that of copper, zinc, and chromium nanoparticles synthesized *via* the same approach. UV-Visible spectra show the λ_{max} of iron nanoparticles at 287 nm. EDX spectra confirmed the absence of impurities; SEM images showed smooth morphology, while XRD diffractions revealed the crystallinity of the particles. The resultant iron nanoparticles were functionalized with *p*-amino benzoic acid (PABA) and anthranilic acid (AA) to enhance their antibacterial activity. Furthermore, bacteria were grown in the presence of non-functionalized and functionalized iron nanoparticles. The inhibition zones in the disc diffusion assay revealed that all the nanoparticles and alum inhibited the growth of *Staphylococcus aureus*, notably compared to the control samples. Furthermore, the antibacterial activity of functionalized nanoparticles was compared to that of non-functionalized nanoparticles. The result showed that anthranilic acid-functionalized iron nanoparticles (AA@Fe) are more effective against Gram-positive *Staphylococcus aureus* than non-functionalized nanoparticles and *para*-aminobenzoic acid-functionalized iron nanoparticles (PABA@Fe). In contrast to the antibacterial activity, PABA@Fe has a good antioxidant activity compared to AA@Fe.

Sustainability spotlight

Engineering of biocompatible nanoparticles aims at fighting the menace of prevailing medication-resistant microorganisms. Methicillin-resistant *Staphylococcus aureus* continuously challenges researchers to discover a potential alternative to marketed drugs. In the present work, anthranilic acid functionalized iron nanoparticles were effectively utilized against *Staphylococcus aureus* which well aligns with UN SDGs-2030, GOAL-3 (Good Health and Well-being).

1. Introduction

Antibacterial medications have been used since their discovery in 1928 to kill or prevent the growth of bacteria and other microorganisms and are responsible for saving millions of lives by making previously fatal illnesses treatable. However, an ongoing issue is that bacterial resistance to these medications has grown significantly over time, as it greatly lowers their efficacy.[1] Bacterial resistance has a wide range of negative consequences in medicine and society. Drug-resistant bacterial infections result in greater drug doses, the inclusion of more toxic therapies, longer hospital stays, and increased mortality.[2,3] Gram-positive *Staphylococcus aureus* (methicillin-resistant) is one of the resistant bacterial strains that easily forms biofilms on prosthetic devices such as pacemakers, heart valves, orthopedic implants, and indwelling catheters. Its biofilms resist antibiotic treatment and represent a significant burden on the healthcare system.[4] It is a frequent human pathogen that causes a number of infections. In addition to general infections like wounds or operative/surgical infections, this bacterium can also cause artificial infection *via* the use of cannulas, and endotracheal tubes.[5,6] The recent advancement in the field of antimicrobial drugs for curing of microbial diseases is one of the wonderful achievements of the pharmaceutical and medical fields.[7] Nevertheless, the potential of pathogenic microorganisms to resist all the ventures of science is incredible. For

[a]Department of Chemistry, University of Malakand, Chakdara-18800, Pakistan. E-mail: sadiq@uom.edu.pk

[b]Department of Chemistry, Bacha Khan University, Charsadda-24420, Pakistan

[c]Department of Biotechnology, University of Malakand, Chakdara-18800, Pakistan

[d]Department of Chemistry, Kyungpook National University, Daegu-41566, South Korea

example, *Staphylococcus aureus* is resistant to marketed antibiotics, *i.e.*, methicillin and vancomycin, due to the presence of the β-lactamase enzyme that hydrolyzes the β-lactam bond and destroys the drug antibacterial potential. In this scenario, researchers always challenge the nasty bacteria by developing various types of bactericides/antibacterial agents.[8] Currently, the emergence of nanotechnology opens new doors to address the formidable challenge posed by microorganisms. It has been one of the most promising strategies for combating microbial resistance in recent times as a drug delivery vehicle. Nanoparticles are successful therapeutic agents, because of their small size (1 to 100 nm) and large surface area with suspended bonds and higher reactivity than their bulk counterparts, which enable efficient interactions with biological systems.[9] Nanotechnology offers fresh methods to combat infections caused by *Staphylococcus aureus* biofilms. Better antibacterial and *anti*-biofilm capabilities have been demonstrated for a number of nanomaterials, nanoparticles (NPs), and drug-encapsulated nanoparticles. Because nanoparticles interact with and penetrate the biofilm matrix more effectively than the current free drug molecules, they have *anti*-biofilm properties and can be applied in the field of bio catalysis and medicine.[10–12] Nanomaterials can be synthesized by different novel approaches (physical, chemical and biological) to obtain nanoparticles with specific shape and size for result oriented applications. Among the reported procedures, chemical approaches, such as precipitation, sol–gel and force hydrolysis, hydrothermal, surfactant mediate/template synthesis, electrochemical and laser pyrolysis, are the simplest and most efficient pathways for producing nanoparticles with a controlled shape and size.[13]

Iron is one of the extensively explored transition metals because of its remarkable crystal structures, low cost, magnetic properties, different oxidation states and eco-friendly nature. Iron nanomaterials are used as safe labeling agents of endothelial progenitor cells in the biomedical field, in immunoassays and magnetic specific site-target drug delivery, and as antimicrobial and antioxidant agents.[14] The antibacterial activity of iron nanoparticles has been extensively studied in human pathogenic bacteria such as *Escherichia coli*[15] and Gram positive *Staphylococcus aureus*.[16] Iron nanoparticles have the potential to replace prevailing antibiotics because they are non-toxic to humans at low quantities. These chemicals have less negative effects than antibiotics and inhibit/stop bacterial growth at lower dosages.[17] Many studies have found that the antimicrobial effects of iron nanoparticles on Gram-positive bacteria *Staphylococcus aureus* and Gram-negative bacteria *Pseudomonas aeruginosa* is due to the reactive oxygen species (ROS) produced by iron nanoparticles which kill bacteria rather than harming non-bacterial cells.[18]

Despite the fact that a large number of antibiotics are available all over the world, bacterial infections still cause a huge number of diseases and mortality. So, we need to develop various types of bactericides in the medical field to inhibit bacterial infections. Thus, this study reports the effectiveness of functionalized iron nanoparticles with PABA and AA for antioxidant activity and antibacterial activity, respectively.

2. Experimental

2.1 Chemicals

Ferrous chloride, ferric chloride, zinc sulfate, copper sulfate, sodium hydroxide, *p*-amino benzoic acid, and anthranilic acid were purchased from Scharlau and Sigma Aldrich and used without further treatment.

2.2 Synthesis of nanoparticles

Iron nanoparticles were synthesized by the microwave-induced precipitation method by taking 100 mL of ferrous chloride and ferric chloride ($FeCl_2$ and $FeCl_3$) (1 : 1.5 M), to which sodium hydroxide (NaOH) (3 M) was added drop-wise. The grayish black mixture was stirred at 80 °C for 4 hours with constant stirring (500 rpm). The mixture was allowed to settle, and the upper water was removed. The residue was washed frequently with distilled water till pH = 7. The resultant black residue was dried overnight in the oven (50 °C) to obtain iron nanoparticles. A similar procedure was adopted for the synthesis of copper, zinc, and chromium nanoparticles.

2.3 Functionalization of nanoparticles

Anthranilic acid (3.36 g) and 4-amino benzoic acid (3.36 g) were refluxed separately with the iron, zinc, copper and chromium nanoparticles for 1 h. The residue was obtained by magnetic decantation and was then rinsed (3 times with DI water) and dried at low temperature.

2.4 Antibacterial activity

2.4.1 Bacterial strain. The activity of nanoparticles against methicillin-resistant *Staphylococcus aureus* was tested.

2.4.2 Disc diffusion assay. Synthesized iron, copper, zinc and chromium nanoparticles were studied for their bactericidal activity using standard microbiology evaluation of the zone of inhibition (ZOI) through the Kirby–Bauer disc diffusion method. A broth culture was prepared by inoculating 4 to 5 colonies from a pure bacterial culture in fresh nutrient broth through a sterilized wire loop. The broth was incubated for 30 min to achieve the turbidity of 0.5 McFarland standard. The turbidity of broth culture was compared with 0.5 McFarland solution. A sterile cotton swab was dipped in the broth and the bacterial suspension was uniformly spread over the surface of an agar plate. Whatman filter paper discs were placed in the right positions on the agar plate with the help of sterile forceps. 7 μL of each sample (30 mg mL^{-1} iron, copper, zinc, and chromium nanoparticles),[19] was added to the respective discs in the plate and incubated for 24 h at 37 °C. 30 mg mL^{-1} ciprofloxacin was used as a control. The test was performed for functionalized iron, copper, zinc and chromium nanoparticles and compared to non-functionalized nanoparticles.

2.5 Antioxidant activity

The antioxidant activity of functionalized iron nanoparticles was investigated using a colorimetric assay based on the discoloration of the oxidized form of 2,2-diphenyl-1-

picrylhydrazyl radical (DPPH) violet to its reduced form yellow. A higher concentration of antioxidants results in a yellower final solution. The absorbance at 517 nm was calculated after a 30-min incubation reaction in 250 L of a 104 M DPPH solution with increasing concentrations of the tested material. The percentage of DPPH inhibition was calculated using the formula.[20]

$$\text{Inhibition (\%)} = \frac{(\text{absorbance of control} - \text{absorbance of sample})}{\text{absorbance of control}} \times 100 \quad (1)$$

2.6 Instrumentation

A spectrophotometer (UV-4000), with spectra ranging from 190 to 1100 nm, and water as the blank were used for studying the optical properties of synthesized iron nanoparticles. FT-IR spectral analysis was used for functional group determination of both non-functionalized and functionalized iron nanoparticles. Scanning Electron Microscopy (SEM) (model: JSM5910, magnification (max): 300 000×, resolving power (max): 2.3 nm) was used to characterize the synthesized NPs morphologically. X-Ray Diffractometry (XRD) (model: JDX-3532, make: JEOL, Japan, voltage: 20–40 kV, current: 2.5–30 mA, X-rays: Cu Kα (wavelength = 1.5418 Å), 2θ range: 0°–90°) was used to determine the crystallinity of the sample. Energy Dispersive X-ray (EDX) (model: JSM-5910) was used for the elemental analysis of the sample.

3. Results & discussion

3.1 Characterization

UV-visible spectra of the synthesized iron and functionalized iron nanoparticles using distilled water as the blank were recorded at room temperature between 200 and 800 nm. The broad absorption peaks of iron and functionalized Fe NPs are observed at ~287 nm and ~280 nm (Fig. 1) due to light absorption and scattering by NPs, indicating the presence of nanoparticles. The blue shift between the two peaks is because of functionalization.

The FT-IR spectra of both iron and functionalized iron nanoparticles are shown in Fig. 2. Iron was observed in both
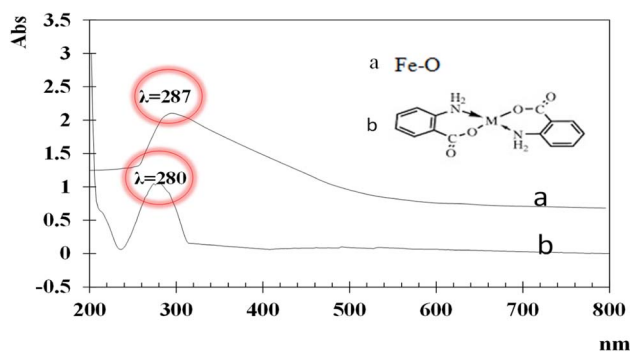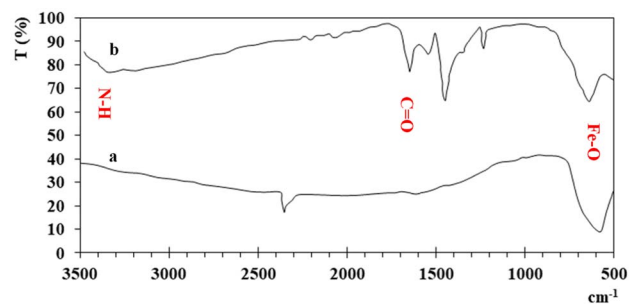

Fig. 2 FT-IR spectra of (a) iron and (b) functionalized iron NPs.

samples with strong absorption in the region 555–570 cm^{-1} and the two peaks in the FTIR spectra of functionalized nanoparticles confirm the presence of carbonyl and amino groups at 1653 and 3344 cm^{-1} respectively.

The elemental composition (Table 1) showed that Fe is a major element in both samples while the presence of carbon shows the functionalization of nanoparticles.

Scanning Electron Microscopy (SEM) thoroughly investigated the morphology of iron nanoparticles. Fig. 3 shows the SEM image and operation parameters used for studying the

Table 1 Elemental analysis of iron and functionalized iron nanoparticles

Non-functionalized iron NPs			Functionalized iron NPs		
Element	Wt (%)	Atomic (%)	Element	Wt (%)	Atomic (%)
O	28.82	55.14	C	5.24	13.11
Fe	70.96	44.65	O	26.62	50.04
Si	0.22	0.21	Si	0.26	0.28
Total	100	100	Fe	67.88	36.56
			Total	100	100
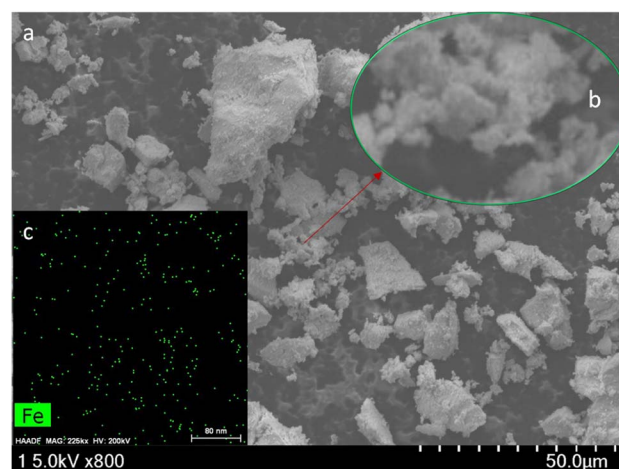
Fig. 3 (a) SEM image, (b) zoomed SEM and (c) elemental mapping of iron nanoparticles.

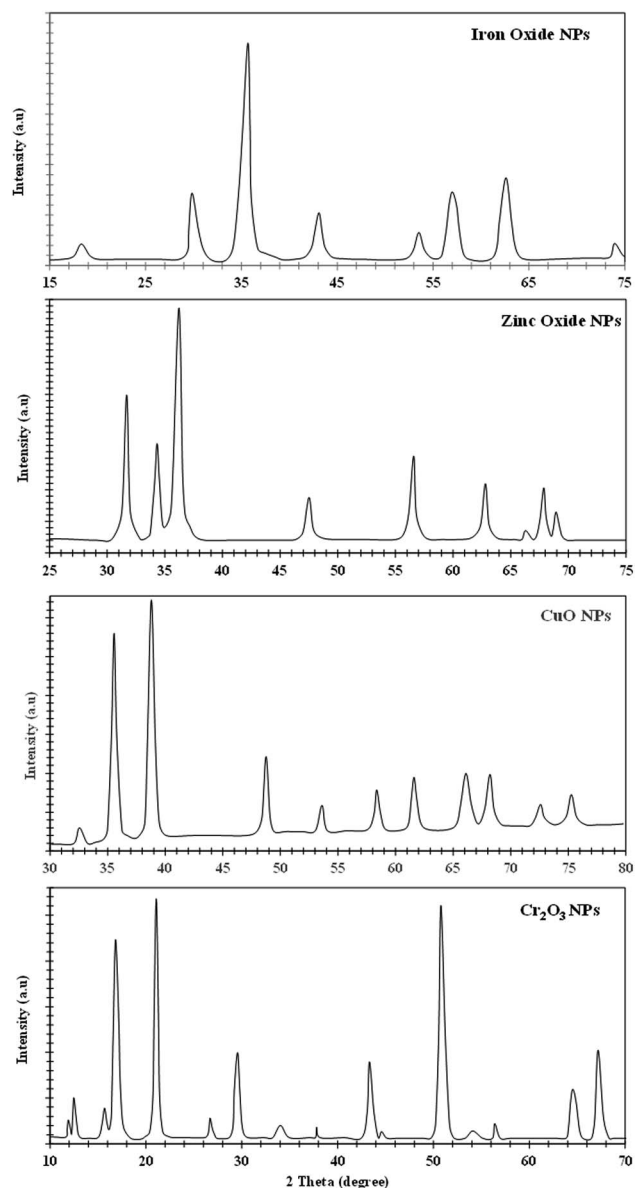Fig. 1 UV-Vis spectra of (a) iron and (b) functionalized iron NPs.

Fig. 4 XRD analysis of iron, zinc, copper and chromium nanoparticles.

morphology of iron nanoparticles. The nanoparticles appear to be cubic and agglomerated. The observed agglomeration of iron nanoparticles could be due to electrostatic interactions between
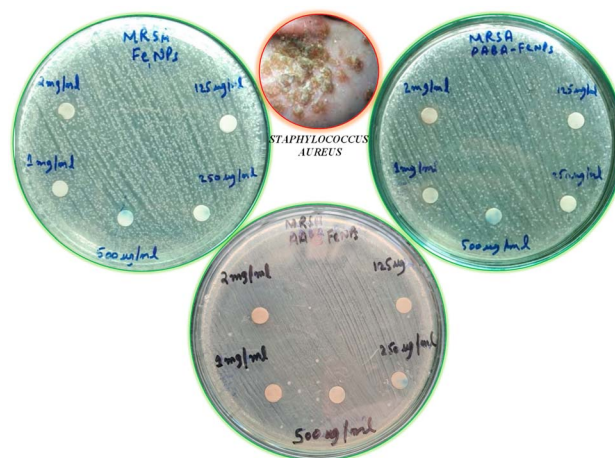

Fig. 5 Effect of concentration on the antibacterial activity of pure and functionalized iron nanoparticles.

nanoparticle surface layers. Furthermore, nanoparticles tend to agglomerate in suspension because of their high surface area-to-volume ratio. The magnified image shows that the particles have a nanometer size.

3.2 X-ray diffractometry (XRD)

The XRD analysis of iron, zinc, copper, and chromium nanoparticles is represented in Fig. 4. The X-ray diffraction pattern of the non-functionalized iron nanoparticles shows various peaks at $2\theta = 17.8°$ (111), $30.0°$ (220), $35.2°$ (311), $43.2°$ (400), $53.2°$ (422), $57.0°$ (511), $62.5°$ (440) and $74.7°$ (533), which shows a crystal plane and cubic crystal geometry and is related to JCPSD card no. (65-3107). Similarly, the XRD pattern for the synthesized zinc NPs (Fig. 4) shows crystal planes and hexagonal crystal geometry according to JCPSD card no. 01-007-2551. The XRD pattern of copper NPs reveals a monoclinic crystal system (JCPDS card no. 45-0937), while the XRD pattern of Cr_2O_3 NPs shows rhombohedral crystal shape geometry according to JCPDS (card no. 74-0326) ascribed to the peaks present. The Scherer equation (intense peaks) was used to calculate the particle size, and the average particle sizes for Fe, Zn, Cu, and Cr NPs were found to be 62 nm, 19 nm, 18 nm, and 17 nm, respectively.

Table 2 Inhibition zone comparisons of functionalized/non-functionalized nanoparticles

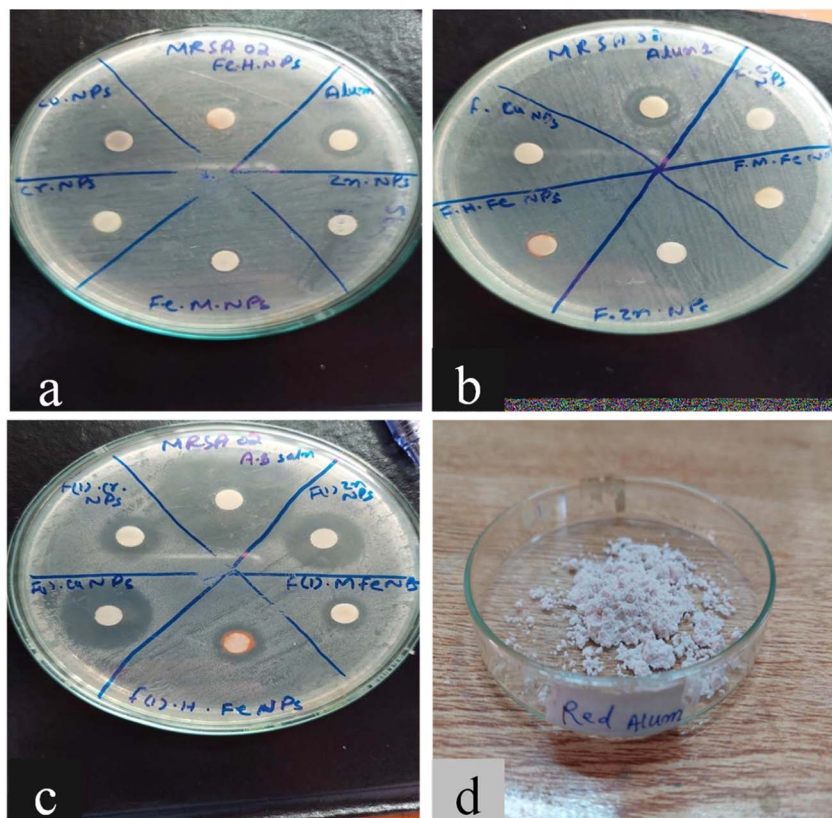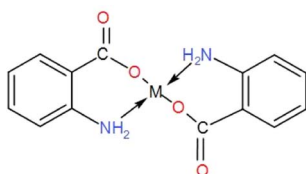| Nanoparticles | Non-functionalized | Functionalized | | Effectiveness (mm) |
		PABA@Fe	AA@Fe (mm)	
Fe^{2+}/Fe^{3+}	8 mm	ND[a]	10	2
Fe^{2+}	ND[a]	ND[a]	11	11
Chromium	ND[a]	ND[a]	13	13
Zinc	ND[a]	ND[a]	18	18
Copper	ND[a]	ND[a]	20	20
Potash alum	12 mm			12
Ciprofloxacin	35 mm			35

[a] Not detected.

Fig. 6 Antibacterial activity of (a) non-functionalized, (b) functionalized (*p*-amino benzoic acid), (c) functionalized anthranilic acid, (d) powder alum.

Scheme 1 Complex of M^{2+} with anthranilic acid (where M^{2+}: Fe, Zn, Cr, and Cu).

3.3 Functionalization of nanoparticles

The surface functionalization of all the synthesized NPs was carried out with PABA, and the observed results are tabulated in Table 2. This is attributed to the fact that the amino group is at the *para* (*trans*) position, and the bonding (coordinate covalent) between the amino group and metal d orbital is not possible due to the phase of plane difference (overlapping gap). The surface functionalization of all the synthesized NPs with anthranilic acid showed enhanced antibacterial activity. This is because an amino group is present in anthranilic acid at the *ortho* position. The complexation of the metal with both the functional groups (COOH & NH_2) is in the plane (aligned),

and the interaction of COOH with the metal takes place easily. At the same time, two coordinate covalent bonds are formed between the metal atom d orbital and NH_2. Hence the metal bi-dentate ligand is formed as depicted in the structure. The complexation of anthranilic acid has a direct role in the enhancement of antibacterial activity due to the interaction of the complex with the extracellular surface. Table 2 shows the zones of inhibition of different metal nanoparticles and anthranilic acid-functionalized metal nanoparticles. Among them, functionalized copper and zinc nanoparticles show the highest inhibition zones, about 20 mm and 18 mm in diameter, while the iron NPs showed activity for both functionalized and non-functionalized nanoparticles with an effectiveness of 2 mm due to the Fenton reaction of mixed Fe^{2+}/Fe^{3+} and the activity is not greatly enhanced by the AA. In comparison, the activity of Fe^{2+} is greatly enhanced by AA due to its complexation capability.

3.4 Antibacterial activity

An antibacterial test for non-functionalized and functionalized nanoparticles against methicillin-resistant Gram-positive *Staphylococcus aureus* was performed using different concen-
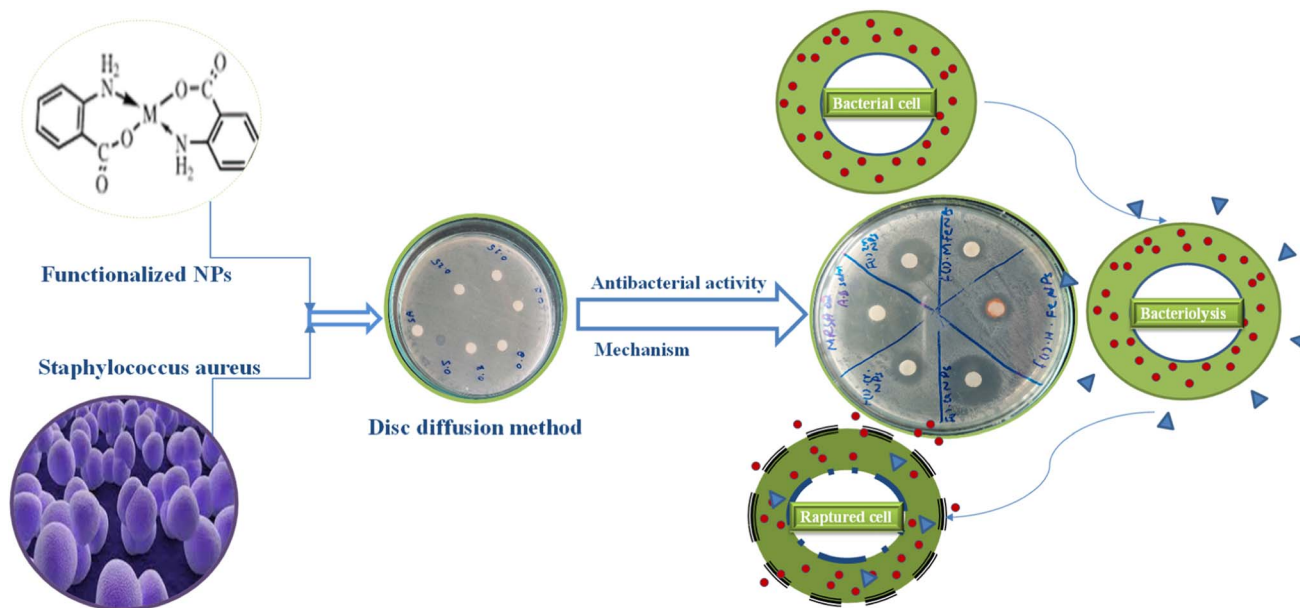
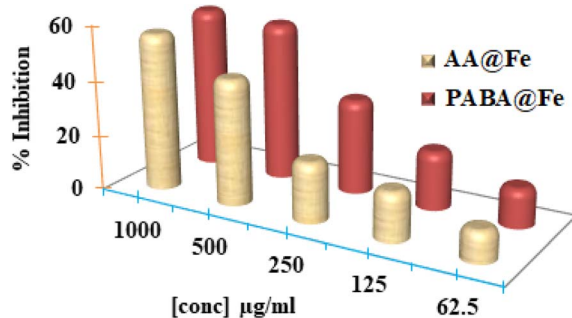Fig. 7 Schematic diagram for nanoparticles antibacterial activity.

Fig. 8 Potential of functionalized iron NPs as an antioxidant.

trations (125 µg mL^{-1} to 30 mg mL^{-1}) as presented in Fig. 5 and 6. Fig. 5 clearly reveals that low concentrations did not show any effective activity against methicillin-resistant *Staphylococcus aureus* therefore 30 mg mL^{-1} (7 µL on the disc)[19] was considered the optimal concentration for efficient activity. The antibacterial activities of PABA@Fe and AA@Fe are presented in Fig. 6b and c, where AA@Fe shows good antibacterial activity compared to PABA@Fe. The most probable reason for the better antibacterial activity of AA@Fe is due to the complexation of M^{2+} with AA, as shown in Scheme 1. The higher antibacterial activity of functionalized nanoparticles is primarily related to their high surface area-to-volume ratio, which allows a larger number of atoms to be present on the surface and the generation of reactive oxygen species (ROS), which inhibits respiratory enzymes. Functionalized nanoparticles act as an antibacterial agent by interacting with the peptidoglycan cell wall and plasma membrane. They also prevent bacterial DNA replication by

interfering with sulfhydryl groups in proteins, and the positive charge of the metal interacts with the negative charge on bacterial cell walls to change the morphology of the cell wall and increase cell permeability or leakage, which ultimately causes cell death, as shown in Fig. 7.

3.5 Antioxidant activity

The antioxidant potential of iron nanoparticles (PABA@Fe & AA@Fe) was determined using DPPH methods. Fig. 8 reveals that the activity is a function of nanoparticle concentration. The increased concentration causes an increase in activity. Both functionalized iron NPs demonstrated 58.125 and 46.625% free radical scavenging activity at 1000 g mL^{-1}, respectively, as shown in Fig. 9. Perhaps, freely available surface functional groups on PABA@Fe are responsible for better antioxidant activity. The strong antioxidant activity achieved using the ABTS method is attributed to the hydrophilicity and better dispersion of materials in an aqueous solution.

In contrast, the results obtained using the DPPH method show lower free radical scavenging capacity. The lower interaction of particles and DPPH free radicals in methanol solution accounts for the lower antioxidant activity in the DPPH method. The antioxidant activity of functionalized iron NPs has been reported to be derived from the surface functional group. The radicals ABTS˙ and DPPH˙ are known to be quenched as the hydroxyl group is converted to H˙. The oxidation process can thus be stopped, preventing the oxidative damage to proteins, nucleic acids, carbohydrates, and lipids. Therefore, in the future, the potential antioxidant activity of iron nanoparticles may be helpful as a tool against cancer and other harmful diseases.
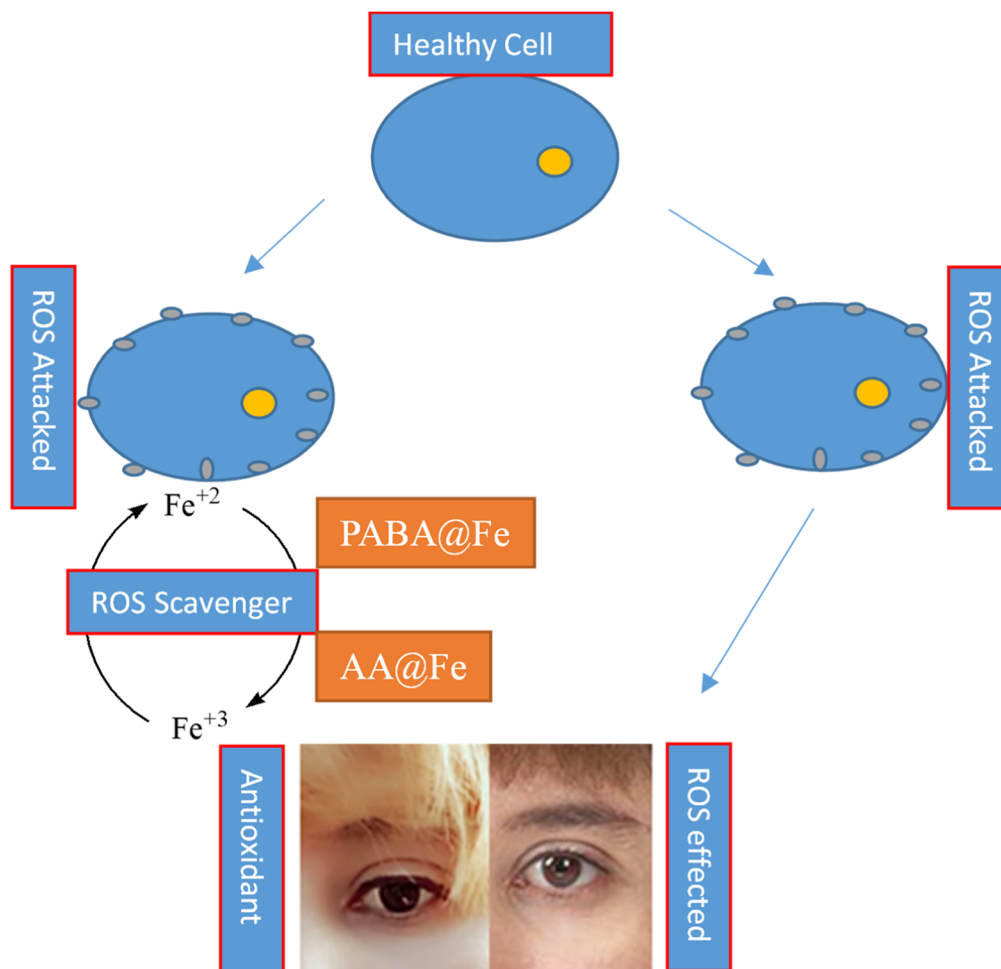
Fig. 9 Schematic diagram for the nanoparticles antioxidant activity.

4.   Conclusion

Nanoparticles of iron, zinc, copper and chromium were synthesized by the microwave-induced precipitation method and successfully functionalized with amino benzoic acid by the reflux method. The growth of methicillin-resistant *Staphylococcus aureus* was significantly suppressed at the highest concentration of nanoparticles and alum compared to the control samples, according to a live/dead evaluation. In addition, the antibacterial activity of all four functionalized nanoparticles was compared to that of non-functionalized nanoparticles. Our results show that nanoparticles functionalized with AA were most effective against Gram-positive bacteria (*Staphylococcus aureus*) compared to non-functionalized NPs and those functionalized with PABA, while the nanoparticles functionalized with PABA show greater antioxidant activity. The current study focuses on the potential use of nanoparticles as antibacterial agents, which can be a good alternative to marketed antibiotics.

Conflicts of interest

The author(s) declare no conflict of interest.

Acknowledgements

References

1 M. J. Hajipour, *et al.*, Antibacterial properties of nanoparticles, *Trends Biotechnol.*, 2012, **30**(10), 499–511.
2 A. J. Huh and Y. J. Kwon, "Nanoantibiotics": a new paradigm for treating infectious diseases using nanomaterials in the antibiotics resistant era, *J. Controlled Release*, 2011, **156**(2), 128–145.
3 D. O. Schairer, *et al.*, The potential of nitric oxide releasing therapies as antimicrobial agents, *Virulence*, 2012, **3**(3), 271–279.
4 M. K. Suresh, R. Biswas and L. Biswas, An update on recent developments in the prevention and treatment of Staphylococcus aureus biofilms, *Int. J. Med. Microbiol.*, 2019, **309**(1), 1–12.

5 M. Grinholc, *et al.*, Bactericidal effect of photodynamic inactivation against methicillin-resistant and methicillin-susceptible Staphylococcus aureus is strain-dependent, *J. Photochem. Photobiol., B*, 2008, **90**(1), 57–63.

6 M. C. Hudson, W. K. Ramp and K. P. Frankenburg, Staphylococcus aureus adhesion to bone matrix and bone-associated biomaterials, *FEMS Microbiol. Lett.*, 1999, **173**(2), 279–284.

7 R. Salomoni, *et al.*, Antibacterial effect of silver nanoparticles in Pseudomonas aeruginosa, *Nanotechnol., Sci. Appl.*, 2017, **10**, 115.

8 Y. N. Slavin, *et al.*, Metal nanoparticles: understanding the mechanisms behind antibacterial activity, *J. Nanobiotechnol.*, 2017, **15**(1), 1–20.

9 R. Singh and J. Lillard Jr, Nanoparticlebased Targeted Drug Delivery, *Exp. Mol. Pathol.*, 2009, **86**, 215–223.

10 R. Y. Pelgrift and A. J. Friedman, Nanotechnology as a therapeutic tool to combat microbial resistance, *Adv. Drug Delivery Rev.*, 2013, **65**(13–14), 1803–1815.

11 K. Ganesh, D. Archana and K. Preeti, Review Article on Targeted Polymeric Nanoparticles: An Overview, *Am. J. Adv. Drug Delivery*, 2013, **3**(3), 196–215.

12 R. P. Dhavale, *et al.*, Chitosan coated magnetic nanoparticles as carriers of anticancer drug Telmisartan: pH-responsive controlled drug release and cytotoxicity studies, *J. Phys. Chem. Solids*, 2021, **148**, 109749.

13 K. Bogunia-Kubik and M. Sugisaka, From molecular biology to nanotechnology and nanomedicine, *Biosystems*, 2002, **65**(2–3), 123–138.

14 M. Arakha, *et al.*, Antimicrobial activity of iron oxide nanoparticle upon modulation of nanoparticle-bacteria interface, *Sci. Rep.*, 2015, **5**(1), 1–12.

15 K.-Y. Yoon, *et al.*, Susceptibility constants of Escherichia coli and Bacillus subtilis to silver and copper nanoparticles, *Sci. Total Environ.*, 2007, **373**(2–3), 572–575.

16 J. P. Ruparelia, *et al.*, Strain specificity in antimicrobial activity of silver and copper nanoparticles, *Acta Biomater.*, 2008, **4**(3), 707–716.

17 N. Beyth, *et al.*, Alternative antimicrobial approach: nano-antimicrobial materials, *J. Evidence-Based Complementary Altern. Med.*, 2015, 246012.

18 H. L. Lumppio, *et al.*, Rubrerythrin and rubredoxin oxidoreductase in Desulfovibrio vulgaris: a novel oxidative stress protection system, *J. Bacteriol.*, 2001, **183**(1), 101–108.

19 S. S. Behera, Characterization and evaluation of antibacterial activities of chemically synthesized iron oxide nanoparticles, *World J. Nano Sci. Eng.*, 2012, **2**(4), 196–200.

20 S. Chattopadhyay, *et al.*, Development of novel blue emissive carbon dots for sensitive detection of dual metal ions and their potential applications in bioimaging and chelation therapy, *Microchem. J.*, 2021, **170**, 106706.